PAPER E1

ULTRASONIC VELOCITIES OF CHALK SAMPLES: INFLUENCE OF POROSITY, FLUID CONTENT AND TEXTURE

Birte Røgen and Ida Fabricius
Environment & Resources DTU, Technical University of Denmark

Peter Japsen and Christian Høier
Geological Survey of Denmark and Greenland (GEUS)

Gary Mavko
Stanford Rock Physics Laboratory

Jacob Mørch Pedersen
Ødegaard A/S

ABSTRACT

The acoustic properties of the pure chalk of the Upper Cretaceous Tor Formation have been studied on core material from the Dan and South Arne fields, Danish North Sea. Detailed investigations were carried out on 56 vertical plug samples with porosities ranging from 14% to 45%, i.e. measurement of P- and S- wave velocities of dry and water-wet samples and microtextural image analysis on backscatter micrographs. Porosity is the primary control on sonic velocities and elastic moduli of chalk with identical pore fluids. For chalk samples dominated by fine carbonate particles (mud) we obtain a well-defined relation between elastic moduli and porosity, which can be modeled using a modified upper Hashin-Shtrikman bound. The trend is defined by a bulk and shear modulus at zero porosity of 54 and 22 GPa, and by a high-porosity end-member at 47%. We find that compaction, grain size distribution, and possibly mineralogy, rather than pore-filling cementation, control the variation of porosity for the samples.

Variations in chalk particle size distribution and the content of non-carbonates influence the relation between elastic properties and porosity for the samples investigated even though the carbonate content is >95%. South Arne samples are found to be stiffer than Dan/Gorm samples for identical porosities e.g. a porosity of 30% corresponds on average to a bulk modulus of 17 GPa and 14 GPa, respectively, for the saturated samples. Conversely, a bulk modulus of 15 GPa

corresponds to porosities of 33% and 28%, respectively, for the saturated South Arne and Dan samples.

The presence of large grains (microfossils) in chalk has a stronger tendency to reduce porosity than to enlarge elastic moduli. We thus find chalk with high content of large grains to have lower elastic moduli for a given porosity than mudstones. The microfossil rich texture found in Dan field samples consequently contributes to the relative softening of these samples for a given bulk porosity.

Gassmann's relations for fluid substitution give valid first order predictions of the elastic properties of dry chalk samples based on observed properties of water-wet samples. The fair agreement between ultrasonic measurements on chalk and Gassmann's relations is interesting because these relations are established for low frequencies, and because this agreement is not always found for clastics. However, we find that the shear modulus is higher for dry plugs than for saturated plugs whereas Gassmann predict the values to be equal, and that this difference is increasing for smaller porosities.

DATA AND METHODS

Selection of samples from the Tor Formation

The investigation has been focused on the matrix properties of the very pure carbonate of the Upper Cretaceous Tor Formation. Altogether, 56 vertical 1½" plugs samples were selected from cores from the Danish oil fields, South Arne and Dan, that are c. 80 km apart (wells A, B, C and M, N, respectively), including two samples from the water zone in the Gorm field (well P). For a discussion of the geology of the Dan and the South Arne field compare with e.g. Jørgensen, 1992, and Mackertich and Goulding, 1999, respectively. The effective stress on the reservoir rocks were found to be about equal for the two fields. The carbonate content of the samples were mostly over 95%, and all samples have quartz present in the non-carbonate fraction. An important factor for the selection of samples was to avoid fractures and if possible, stylolites. A variation in porosity, permeability and depth was sought in order to study the effect of variation in primary and secondary texture. The porosity ranges covered by the samples are from 19% to 32% for the 27 Dan/Gorm samples and from 14% to 45% for the 29 South Arne samples. The plugs were soxhlet cleaned and dried at 110 ^{o}C.

Microtextural analysis of chalk samples by image analysis

The image analyses for this study were performed at DTU on backscatter micrographs (BSE images) following the method for determination of grain size distribution described in Røgen, Gommesen and Fabricius (in press), and the method for determination of specific perimeter described in Borre, Lind and Mortensen (1997).

Grain size distributions presented were estimated in a two-dimensional plane. One square cm size, vertically oriented samples were prepared for imaging in a Phillips XL20 Scanning Electron Microscope at DTU. The samples were impregnated with epoxy and polished. A standard imaging procedure was followed. An overview image of the sample was taken to check for inhomogeneities. Then four image fields were chosen along the centreline in vertical direction with spacing of 2 mm.

Each image field is represented by two images. One image at large magnification (representing 60 µm x 80 µm), only representing chalk matrix, insoluble residue, and matrix porosity. The second image as a concentric image at 10 times smaller magnification (representing 600 µm x 800 µm) showing microfossils, chalk clasts, and shell debris as well as intraparticular and moldic porosity, but not resolving the matrix. From combination of information from each of the magnifications and under the assumption of a homogeneous matrix, we obtain information corresponding to 100 images of the large magnification at each image field of the small magnification. In this study grains are defined as particles>316 μm^2 (microfossils and shell debris).

Ultrasonic measurements on chalk samples

Conventional core analysis and determination of ultrasonic P- and S- velocities for plug samples at reservoir overburden pressure was carried out at GEUS Core Laboratory. The transit time for the P- and S-wave was measured by a Tektronix Model TDS3012 2-channel digital-phosphor oscilloscope, which was connected to a PAR spike-generator and a modified AutoLab 500 Ultrasonic core holder from New England Research. The P- and S-wave transducer has a center frequency at 700 kHz. P- and S-waves were measured on dried and fully saturated plugs (tap water) at 25, 50 and 75 bar hydrostatic confining pressure. The confining pressure was increased continually to the next pressure step during a time period of 30 minutes using a SP-5400 high-pressure pump system from Quizix. The P- and S-wave data were saved digitally for later analysis. When unloading the core holder, the confining pressure was decreased continually from 75 to 0 bar during a time period of 1½ hour.

The system delay time was determined by measuring transit time without any plugs and on 3 aluminum plugs with different lengths. The ultrasonic velocity was calculated from the reading of the transit time, the sample length and the system delay time. The typical error was found to be less than ± 40 m/s for P-waves and ± 15 m/s for S-waves, but reaching ± 120 m/s for P-waves and ± 45 m/s for S-waves for bad-quality signals. The largest errors were found to be due to difficulties in reading the transit time.

Re-measurement of dry samples

Re-measurements of three dry plugs at room moisture resulted in velocities close to those estimated in the original experiment, considering the limited accuracy of the travel time readings. However, a slight reduction of both P- and S-velocities are observed (0-0.04 km/s), and these changes are in a direction in agreement with the Gassmann predictions. Adjustment of the plugs to room conditions in future measurements is thus likely to prevent them from being 'overcooked', i.e. very dry – a state for which the Biot-Gassmann theories perform poorly (see Mavko et al. 1998). The observed changes are however small and do thus only seem to be a contributor to the limited scatter of the S-velocities.

RESULTS

Loss of porosity due to compaction

A general porosity loss with depth is observed for the chalk samples from both Dan and South Arne fields (Figure 1). This trend reflects mechanical compaction of the chalk due the increase of effective stress (compare Scholle, 1977; Borre and Fabricius, 1998; Japsen, 1998). However, the large variation in porosity for a given depth reflects textural variations of the chalk (compare Fabricius et al., 2000). We will investigate the increase of the moduli of the chalk samples as porosity is reduced by compaction, and the secondary influence of textural variations.

Influence of porosity on elastic properties

Mean P-velocity measured on 56 dry plugs was 3.19 km/s, and 3.17 km/s on 34 saturated plugs, whereas the mean S-velocity measured on 56 dry plugs was 1.97 km/s, and 1.67 km/s on 33 saturated plugs (75 bar confining pressure). This variation results in a mean V_P-V_S ratio of 1.61 for the dry plugs and 1.90 for the saturated plugs. A negative correlation between porosity and both P- and S-velocity (and bulk and shear modulus) was observed for both dry and saturated samples (Figures 2, 3). Distinct relationships between V_P and V_S were observed for both dry and saturated samples (Figure 4). The V_P-V_S ratio converges towards 1.8 and 1.6 at zero porosity for the dry and saturated samples, respectively, as estimated by linear regression analysis of the data. The value for calcite is 1.9 (Mavko et al. 1998).

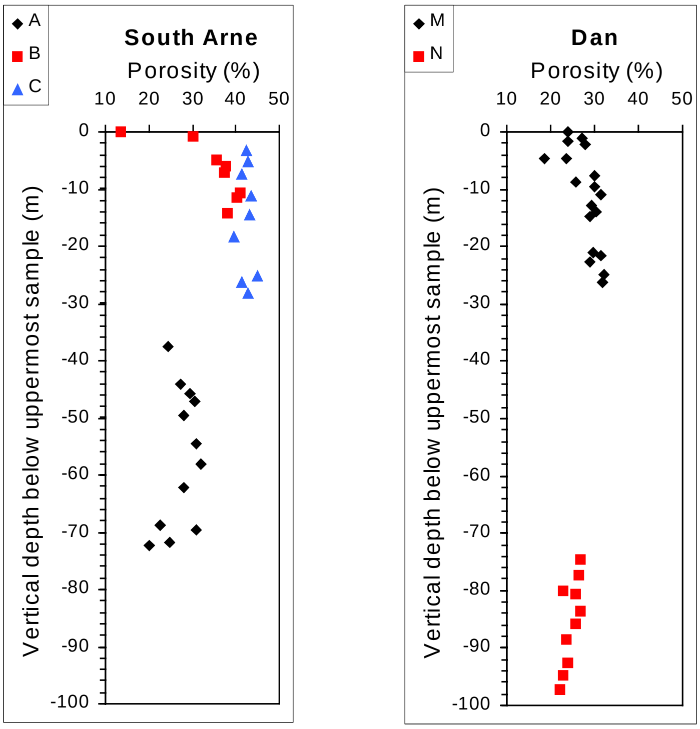

Figure 1. Porosity vs. vertical depth for the South Arne and Dan fields. The depth is relative to the uppermost sample in each field. Symbols for wells A, B, C, M and N are indicated. A porosity loss with depth due to compaction is observed for both fields, but also large deviations from this overall trend are observed for both fields.

A clear difference was observed between results from the two fields in that e.g. the bulk modulus for plugs at 30% porosity is found to be higher for the South Arne Field than for those from the Dan/Gorm Field - or for a given stiffness, the porosity of the South Arne plugs is higher than for those from Dan/Gorm Field). An identical bulk modulus of 15 GPa corresponds to a porosity of 28% for the Dan/Gorm data set, but to 33% for the South Arne data set when substituting into the results of the linear regression for saturated plugs. How this difference between the two fields may be related to textural differences is investigated later in this paper.

A "mudstone trend" has been modeled as a modified upper Hashin-Shtrikman bound to fit the trend between P-wave modulus and porosity for dry samples with less than 10% of large grains relative to solids (Figure 5). Samples with less than 10% grains are dominated by the sorting between fine and coarse matrix particles. The model is defined by a bulk and a shear modulus at zero porosity of 54 GPa and 22 GPa, a high porosity end-member at 47%, and a bulk modulus of the fluid of 2.2 GPa. The modeled moduli equal the moduli of calcite with 30 % clay with water as pore filling fluid, which of cause is not a realistic mixture, but a best fit.

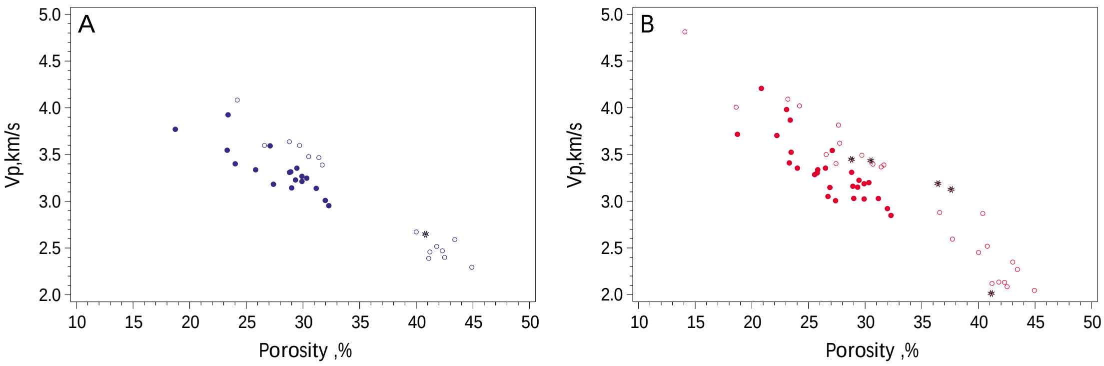

Figure 2. Plot of V_P versus porosity for all samples (75 bar confining pressure). A: Saturated samples, B: dry samples. Solid circles: Dan/Gorm samples, open circles: South Arne samples, asterix: uncertain value. Note the different trends for the Dan/Gorm and the South Arne samples.

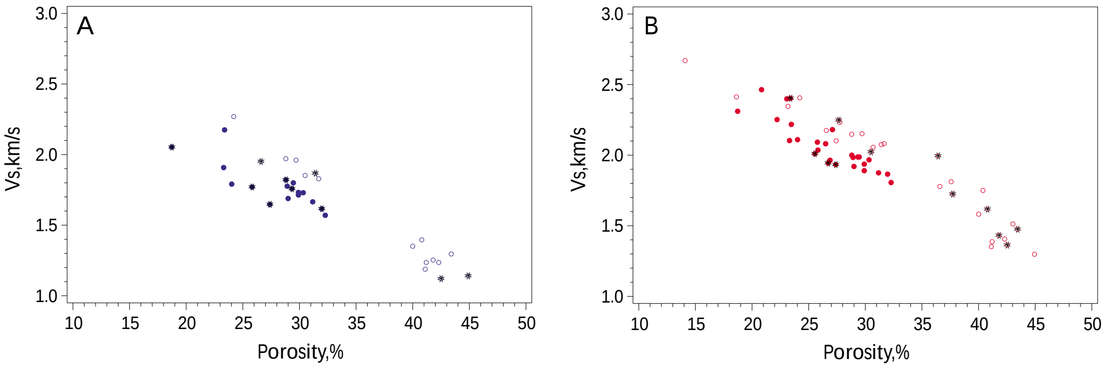

Figure 3. Plot of V_S versus porosity for all samples (75 bar confining pressure). A: Saturated samples, B: dry samples. Solid circles: Dan/Gorm samples, open circles: South Arne samples, asterix: uncertain value. Note the different trends for the Dan/Gorm and the South Arne samples.

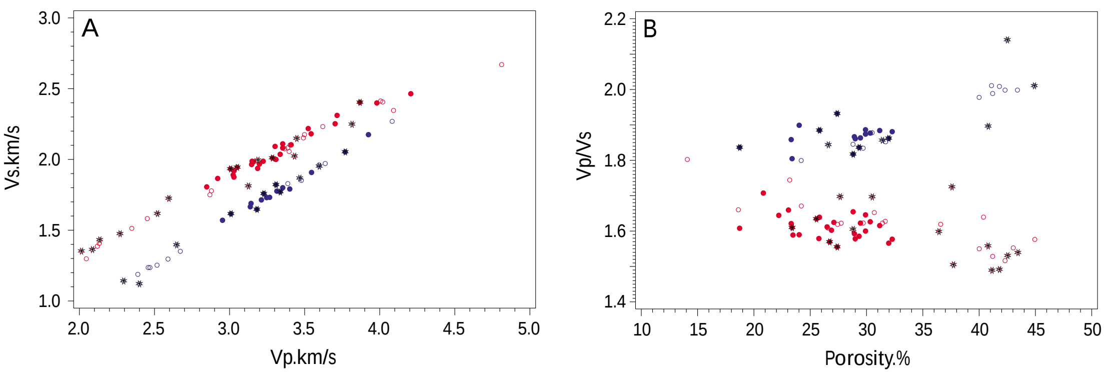

Figure 4. Plot of the relation between V_P and V_S for all samples (75 bar confining pressure). A: V_S versus V_P, B: V_P-V_S ratio versus porosity. Solid circles: Dan/Gorm samples, open circles: South Arne samples, asterix: uncertain value. red symbols: dry samples, blue symbols: saturated samples. Note the distinct relations between V_P and V_S for dry and saturated samples.

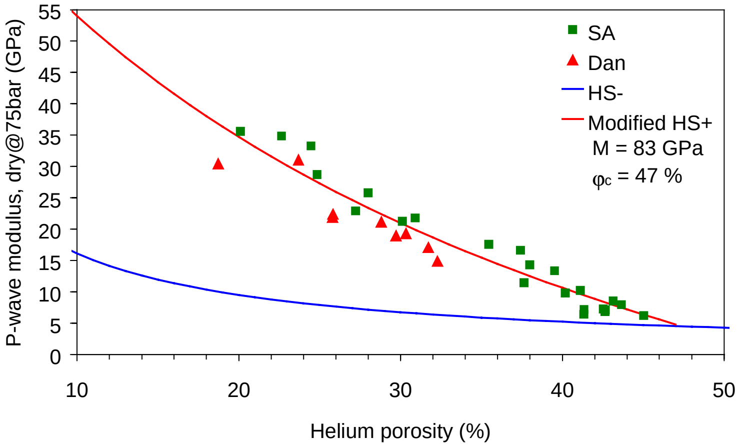

Figure 5. Modified upper Hashin-Shtrikman model and P-wave modulus versus helium porosity for dry mudstone samples (less than 10% grains) measured at 75 bar. The trend is defined by a bulk and a shear modulus at zero porosity of 54 GPa and 22 GPa, and a high porosity end-member at 47%. Bulk modulus of the fluid is 2.2 GPa.

Textural influence on elastic properties

Influence of large grains (microfossils)

Dan field samples have lower sonic velocities for a given porosity than most South Arne field samples (Figures 2, 3). We can estimate if this difference is due to variation in the amount of large grains (microfossils) by relating the elastic properties to the matrix porosity rather than to the laboratory measured Helium porosity (Figure 6). The data points for the two fields move closer when plotted against matrix porosity, and thus the matrix porosity appears to be important for the stiffness of the samples whereas the large grains tend to be passive (Figure 7). The Dan field samples do, however, still tend to be softer than the South Arne field samples, implying that the amount of grains is not the only factor separating the elastic properties of the samples from the two fields. Few samples appear stiffer when plotted against matrix porosity, and this is due to the pore filling cement of these samples (water zone, Gorm field).

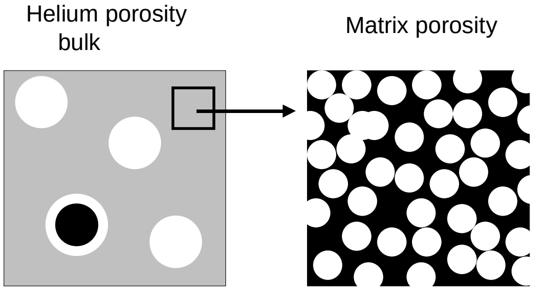

Figure 6. Conceptual model defining matrix porosity as black pore space relative to image size in the right image (high magnification). Large grains and large pore space are defined in left image (low magnification) representing the total sample. Helium porosity is defined in the left image as sum of large porosity and small porosity. Small porosity represents the small pores known from the right image, but relative to the image size of the left image.

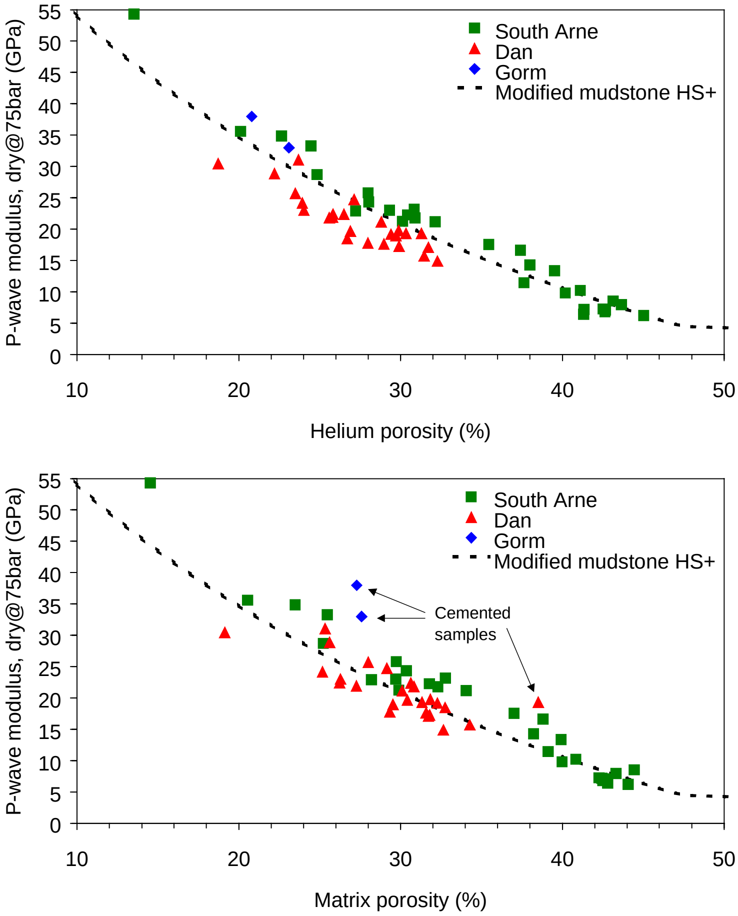

Figure 7. P-wave modulus for dry samples at 75 bar versus helium porosity in the upper cross plot, and versus matrix porosity in the lower cross plot. Field indicated with symbols together with the upper Hashin-Shtrikman model from Figure 5. With an overlap, Dan field samples have lower P-modulus for a given porosity than most South Arne field samples (upper Figure). In the lower figure the helium porosity is replaced by the matrix porosity to subtract the influence from large grains (see Figure 6). Here the samples from the two fields move closer, but the Dan samples still tend to be softer than the South Arne samples, and this suggests that the amount of grains is not the only factor differing the two fields. Few samples appear stiffer when plotted against matrix porosity, implying that these samples have pore filling cement present (water zone, Gorm field).

Influence of hollow versus filled microfossils

Microfossils appear hollow in some and filled with cement in other samples in backscatter micrographs (Figure 8). Samples with filled microfossils do not necessarily have pore filling cement in the matrix. When grains are taken into account by relating moduli to the porosity of the matrix, we observe that samples with and without grains follow the same porosity trend in P-modulus (Figure 7), but that the presence of hollow microfossils has a tendency to lower the stiffness of the sample (Figure 9).

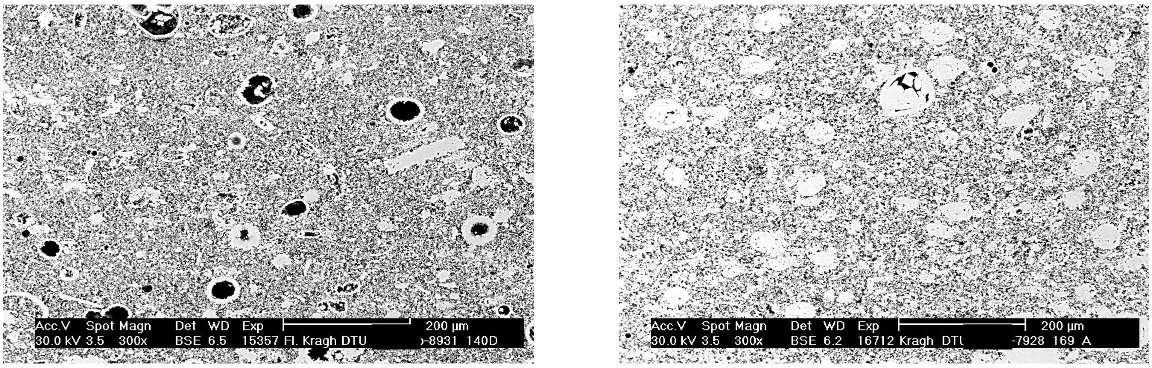

Figure 8. Backscatter micrograph of a sample with hollow microfossils (left) and sample with cemented microfossils, but no pore filling cement in the matrix (right). The images represent 800 µm by 600 µm, and the matrix particles are not resolved. Large grains are seen as white areas, and large porosity within microfossils as black areas.

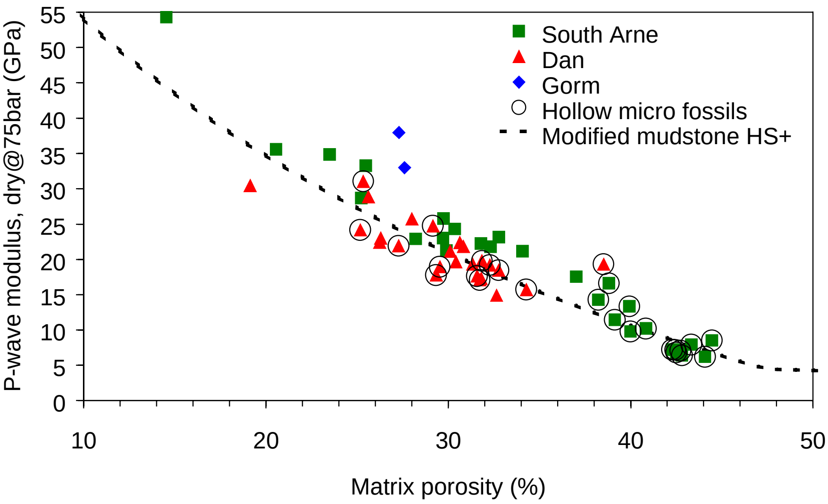

Figure 9. P-wave modulus versus matrix porosity for dry samples at 75 bar. Samples with hollow microfossils are marked with a circle (see figure 8). Field indicated. Presence of hollow microfossils has a tendency to lower the stiffness of the sample.

Influence of pore fluid on elastic properties

Gassmann prediction of dry rock properties from data for the saturated rock

We can predict the elastic properties of the dry rock from data for the saturated rock using Gassmann's relations (see Mavko et al. 1998, p. 170):

$$K_{dry-G} = \frac{K_{sat}\left(\frac{K_0 \cdot \phi}{K_{fl}} + 1 - \phi\right) - K_0}{\frac{K_0 \cdot \phi}{K_{fl}} + \frac{K_{sat}}{K_0} - 1 - \phi}, \qquad \mu_{sat} = \mu_{dry}$$

where $K_{dry\text{-}G}$ = effective bulk modulus of dry rock predicted from Gassmann's relations, K_{sat} =effective bulk modulus of rock with pore fluid, K_0 = bulk modulus of mineral material making up rock, K_{fl} = effective bulk modulus of pore fluid, ϕ = porosity, μ_{dry} = effective shear modulus of dry rock, μ_{sat} = effective shear modulus of rock with pore fluid

We chose to predict K_{dry-G} from measured values of K_{sat}, μ_{sat} and ϕ with K_0=77 GPa for calcite and K_{fl}=2.25 for water. We can now predict the P- and S-velocities for the dry rock, $V_{P-dry-G}$ and $V_{S-dry-G}$:

$$V_{P-dry-G} = \sqrt{(K_{dry-G} + \mu_{sat}) / \rho}, \qquad V_{S-dry-G} = \sqrt{\mu_{sat} / \rho},$$

where $\rho=(1-\phi)\cdot\rho_{gr}$ is the density [g/cm^3] of the dry rock; ρ_{gr} is the measured grain density for the rock. We can compare the Gassmann predictions for the dry rock with data measured on dry rock samples (e.g. K_{dry}, μ_{dry}, V_{P-dry}, V_{S-dry}). We can compute the measured difference, ΔP between any of the parameters (referred to as P in the following) for the dry plugs, P_{dry}, relative to those for the saturated plugs, P_{sat}:

$$\Delta P = P_{dry} - P_{sat}$$

and the predicted difference, ΔP_G between the parameters predicted for the dry plugs, P_{dry-G}, relative to those measured for the saturated plugs:

$$\Delta P_G = P_{dry-G} - P_{sat}$$

Finally, we can calculate a 'Gassmann Index', I_G [%] to describe to which degree we observe the change predicted by Gassmann theory by dividing the measured difference with predicted difference:

$$I_G = \Delta P / \Delta P_G \cdot 100$$

Gassmann prediction and data

The shear modulus for the dry and saturated plug is predicted to be unchanged, but we observe an increasing difference for the smaller porosities (Figure 10A, B). The bulk modulus has about the same variation for both states, but the predicted increasing difference with reduced porosity is not measured. The predicted smaller difference for the South Arne samples (due to their greater stiffness) is also not recorded.

The difference for in S-velocity for the dry and saturated plug is predicted to be reduced with smaller porosities, but we observe an almost increasing difference (Figure 10C, D). The difference for the P-velocities is observed to be reduced for the smaller porosities because of corresponding changes in the bulk and shear modulus are counteracting in the computation of V_P.

The mean error is only 0.20 GPa when predicting K_{dry} from Gassmann's relation and data for the saturated sample. The relative error is 4% compared to the predicted difference between the saturated and dry sample. However, Gassmann's relations predict μ_{sat} - μ_{dry} = 0, whereas the measured difference is 0.56 GPa, e.g. increasing values of μ_{dry}. This results in a mean error of 0.07 km/s in the prediction of both V_P and V_S. So where we expect V_P to decrease with a mean value of 0.22 km/s we observe only a drop of 0.15 km/s, whereas we expect V_S to increase with 0.14 km/s and observe 0.21 km/s. Expressed as the ratio between the measured and the predicted difference we observe only 68 % of the drop in V_P predicted by Gassmann, whereas the increase in V_S is 161 % of that predicted by Gassmann ('Gassmann Index'). The main reason for these differences, is that μ is found to be higher for the dry plug than for the saturated plug whereas Gassmann predict the values to be equal. The Gassmann prediction of K is in average quite accurate.

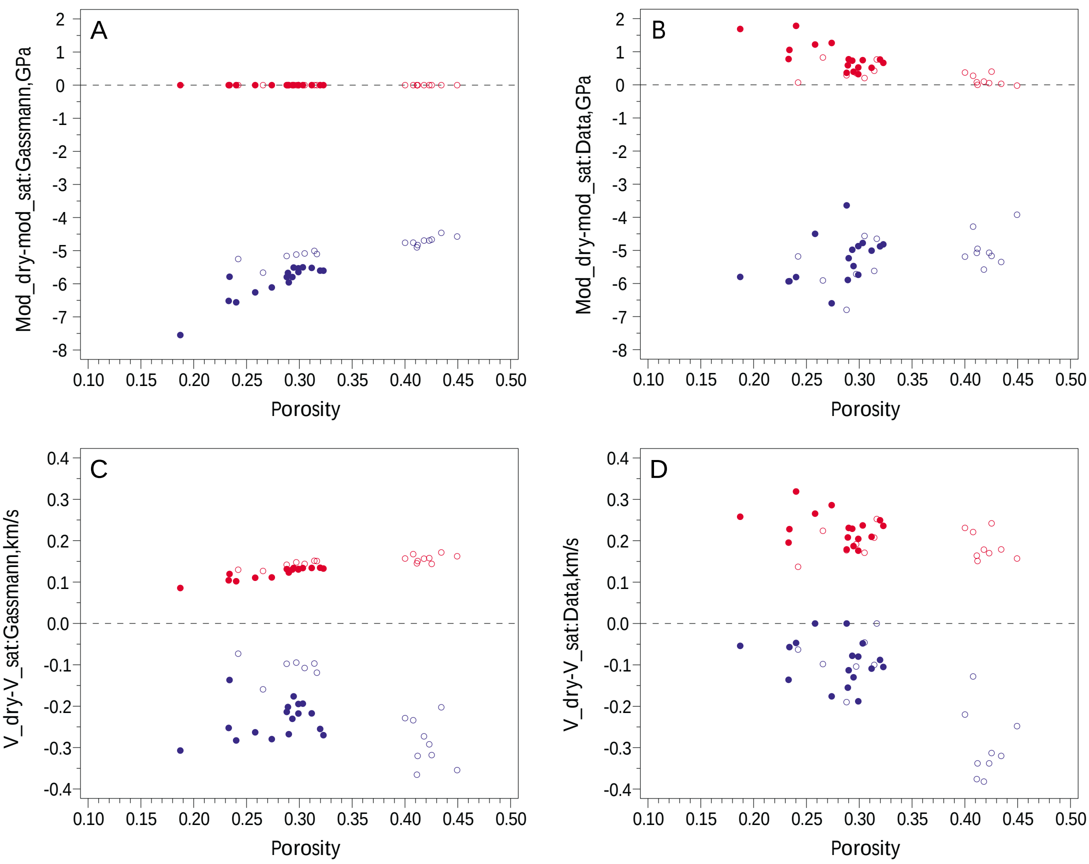

Figure 10. Difference between properties for dry and saturated samples versus porosity (75 bar confining pressure). A and B: $Mod_{dry} – Mod_{sat}$ for both bulk and shear modulus (blue and red, respectively). C and D: $V_{dry} – V_{sat}$ for both P- and S-velocities (blue and red, respectively). Figures A and C show the Gassmann prediction (from wet to dry) of the difference between parameters for dry plugs relative to those measured for saturated plugs. Figures B and D show the measured difference between parameters for dry and saturated plugs. The Gassmann prediction is in general agreement with the measured differences, but it is found that the main reason for the differences is that shear modulus is higher for the dry plug than for the saturated plug whereas Gassmann predict the values to be equal. Solid circles: Dan/Gorm samples, open circles: South Arne samples, asterix: uncertain value.

DISCUSSION AND CONCLUSIONS

A modified upper Hashin-Shtrikman model was defined as “mudstone trend” for data from dry samples with less than 10% grains to describe the increase in elastic moduli during reduction in porosity due to compaction. The model is given by a bulk and shear modulus at zero porosity of 54 and 22 GPa, and by a high-porosity end-member at 47%. This is somewhat lower low-porosity end members, but still comparable to the chalk HS models established for log data by Walls et al., 1998 (65 and 27 GPa, 40%) and by Japsen et al., 2000 (62 and 20 GPa, 45%). A better understanding of these differences awaits further studies, e.g. of the porosity reducing processes in chalk.

Porosity estimated from sonic data is 5 %-units higher for chalk samples from the South Arne Field than from the Dan Field for porosities around 30%. This result is surprising considering the high carbonate content of all samples, and we suggest the difference to be related to textural differences between the chalk at the two locations. Presence of grains in a mud-supported sample does not contribute to the stiffness of the sample, but reduces porosity. However, presence of hollow grains (microfossils) may result in softer samples. The samples investigated have high contents of carbonate, mostly over 95%, and all samples have quartz present in the non-carbonates. This leaves very little amount of clays, but preliminary investigations suggest that the mineralogy of the clay has about the same influence on the stiffness of the samples as the influence from large grains. Clays appear to have different effect depending on clay mineralogy, and this will be further investigated in an ongoing research program.

The mean change in P- and S-velocities when going from saturated to dry samples was found to be a drop of 0.15 km/s and an increase of 0.21 km/s, respectively. These changes correspond to a mean decrease in the bulk modulus of 5.24 GPa and an increase in the shear modulus of 0.56 GPa. These changes correspond only to 68% of the drop in V_P predicted by Gassmann’s relations, whereas the increase in V_S is 161% of that predicted by Gassmann. The main reason for these differences is that shear modulus is higher for the dry plug than for the saturated plug whereas Gassmann predict the values to be equal. This difference is found to be increasing for smaller porosities. The Gassmann prediction of bulk modulus is in average quite accurate. The fair agreement between high frequency ultrasonic measurements on chalk and Gassmann’s relations is interesting because these relations are established for low frequencies, and because this agreement is not always found for clastics. It is frequently assumed that Gassmann should not be used for ultrasonics, because of velocity dispersion effects such as squirt dispersion due to microcracks and heterogeneity of pore stiffness. Maybe the relative applicability of Gassmann observed here is related to the low permeability of the chalk.

ACKNOWLEDGEMENTS

The present paper presents results from the research project 'Rock Physics of Chalk' (1998-2000). The project aimed at establishing a better understanding of the relationship between porosity and velocity of chalk to improve interpretation of seismic data in terms of reservoir parameters. The project was funded by the Danish Energy Research Programme, EFP-98. The project was further strengthened by collaboration with the operators of the Dan and the South Arne field, Mærsk Oil and Gas A/S and Amerada Hess A/S, respectively. The operators placed core material, as well as log and seismic data from recent wells at the disposal for the project.

The investigations continues within the project 'Rock Physics of Impure Chalk Sequences' (2001-2002) which is funded by the Danish Energy Research Programme, EFP-01, Amerada Hess A/S and DONG E&P. This project will focus on the influence of the presence of silica and clay on the acoustic properties of chalk.

Both projects are carried out in co-operation between the Geological Survey of Denmark and Greenland (GEUS), the Technical University of Denmark (DTU), Ødegaard A/S and Gary Mavko, Stanford University.

REFERENCES

Borre, M. and Fabricius, I., 1998, Chemical and mechanical processes during burial diagenesis of chalk: an interpretation based on specific surface data of deep-sea sediments: Sedimentology, **45**, 755-769.

Borre, M., Lind, I. and Mortensen, J., 1997, Specific surface as a measure of burial diagenesis of chalk. Zentralblatt für Geologie und Paläontologie 1997, 1071-1078.

Fabricius I., Røgen B., Borre M. and Japsen P., 2000, Sonic velocities and microtexture of chalk. In: Stanford Rockphysics & Borehole Geophysics Project Annual Report, **75**, 1-13.

Japsen, P. 1998, Regional velocity-depth anomalies, North Sea chalk. A record of overpressure and Neogene uplift and erosion: AAPG Bulletin **82**, 2031-2074.

Japsen, P., Wagner, H., Gommesen, L. and Mavko, G., 2000, Rock physics of Chalk: modeling the sonic velocity of the Tor Formation, Danish North Sea. In: EAGE 62nd Conference and Technical Exhibition, Glasgow, Scotland, 29 May - 2 June 2000, 1-4. Houten: EAGE.

Jørgensen, L. N., 1992, Dan Field; Denmark, Central Graben, Danish North Sea. In: Foster, N.H. and Beaumont, E.A. (eds) AAPG Treatise of Petroleum Geology, Atlas of Oil and Gas Fields. AAPG, Tulsa, 199-218.

Mackertich, D. S. and Goulding, D. R. G., 1999, Exploration and appraisal of the South Arne field, Danish North Sea. In: Fleet, A.J. and Boldy, S.A.R. (eds) Petroleum Geology of Northwest Europe: Proceedings of the 5th Conference. Geological Society, London, 959-974.

Mavko, G., Mukerji, T. and Dvorkin, J., 1998, The rock physics handbook: Cambridge University Press, Cambridge.

Røgen, B., Gommesen, L. and Fabricius, I. L., in press: Grain size distributions of Chalk from image analysis of Electron Micrographs: Computer and Geosciences.

Scholle, P.A., 1977, Chalk diagenesis and its relation to petroleum exploration; oil from chalks, a modern miracle? AAPG Bulletin, **61**, 982-1009.

Walls, J. D., Dvorkin, J. and Smith, B. A. 1998, Modeling seismic velocity in Ekofisk Chalk. In: Proceedings from SEG annual conference and exhibition. SEG, Tulsa, 1016-1019.